J Neuropathol Exp Neurol
Vol. 77, No. 10, October 2018, pp. 929–941
doi: 10.1093/jnen/nly072

ORIGINAL ARTICLE

An Intimate Role for Adult Dorsal Root Ganglia Resident Cycling Cells in the Generation of Local Macrophages and Satellite Glial Cells

Anand Krishnan, PhD, Sudha Bhavanam, MSc, and Douglas Zochodne, MD, FRCPC

Abstract

The intricate interactions between neurons, glial, and inflammatory cells within peripheral ganglia are physiologically important, but not well explored. Here, we show that adult dorsal root ganglia (DRG) contain populations of self-renewing cells, collectively referred as DRG resident cycling cells (DRCCs), that are active not only in "quiescent" ganglia but also accelerate their turnover in response to distal axotomy. An unexpected proportion of DRCCs were resident macrophages. These cells closely accompanied, and aligned with recycling satellite glial cells (SGCs) that were juxtaposed to sensory neurons and possessed stem cell-like properties. Selective inhibition of colony stimulating factor 1 receptor prevented the local proliferation of macrophages. Interestingly, DRCC turnover was accompanied by apoptosis at later intervals indicating a balanced cellular milieu in the DRGs. These findings identify a complex interactive multicellular DRG microenvironment supporting self-renewal of both macrophages and SGCs and its potential implications in the overall response of adult DRGs to injury.

Key Words: Brdu, Dorsal root ganglia, Ki67, Proliferation, Resident macrophages, Satellite glial cells.

INTRODUCTION

Peripheral ganglia or dorsal root ganglia (DRG) consist of mature neurons, satellite glial cells (SGCs), microvessels and macrophages. Interestingly, a population of less characterized actively cycling cells, herein referred as DRG resident cycling cells (DRCCs), is also found in the DRG. DRCCs rise in number after axotomy but it is unclear which DRG constituent cells are actively repopulated by the DRCCs, and whether macrophages or SGCs are involved (1).

SGCs are close partners of DRG neurons. They get activated after nerve injury, tightly pack each other to form outer "rings" around individual injured sensory neurons, and express GFAP and other critical growth signaling molecules (2, 3). Whether the "rings" of SGCs represent repopulating SGCs is not clearly understood. Although previous studies speculated, based on the characteristic interneuronal locations of the SGCs, that nerve injury induced-DRCCs form repopulating SGCs, a clear demonstration of this using specific immunological markers is lacking (4). In this work we address whether SGCs self-renew in adult DRGs using specific immunological markers.

An intricate involvement of immune cells on neuronal response to injuries and other neuropathies has been recognized much earlier (4). Follow-up studies revealed multifaceted roles for macrophages on neuron regeneration, degeneration, and pain modulation in the peripheral nervous system (5–8). Recent studies showed that various phenotypes of macrophages, the proinflammatory M1 and anti-inflammatory M2 subtypes, exist in the nervous system accounting for their multiple functions (9). However, an exact mechanism for the generation of multiple phenotypes of macrophages in the adult DRGs in response to changing local demand is not recognized. Local proliferation of resident macrophages was demonstrated in lung and atherosclerotic lesions, suggesting a potential intrinsic mechanism to meet their growing local demand (10–12). In this study, we examined this possibility in intact and axotomized DRGs.

Commonly, cell proliferation in vivo is identified solely based on systemically administered Brdu incorporation in cells. However, systemic administration of Brdu labels newborn cells in a nonsite-specific manner and may fail to discriminate locally repopulating cells from newborn cells that migrate from distant territories. Here, we used both Brdu incorporation and expression of Ki67 to identify DRCCs in adult DRGs. The advantage of Ki67 is that its role as a transient marker renders its expression only in cells that are in an active division phase. Since active division and cell migration do not happen concurrently, Ki67 expression differentiates DRCCs from infiltrating newborn cells. Using these markers in our multiple experimental models, we demonstrate here that

From the Neuroscience and Mental Health Institute (NMHI) (AK, DZ); Division of Neurology, Department of Medicine (AK, DZ);Alberta Diabetes Institute (AK, DZ); and Division of Laboratory Medicine and Pathology, Department of Medicine, University of Alberta, Edmonton, Alberta, Canada (SB).

Send correspondence to: Douglas Zochodne, MD, FRCPC, Division of Neurology, Department of Medicine, University of Alberta, 7-132 Clinical Sciences Building, Edmonton, Alberta T6G 2B7, Canada; E-mail: zochodne@ualberta.ca

This study was supported by an operating grant from the Canadian Institutes of Health Research (FRN15686).

The authors have no duality or conflicts of interest to declare.

Supplementary Data can be found at academic.oup.com/jnen.

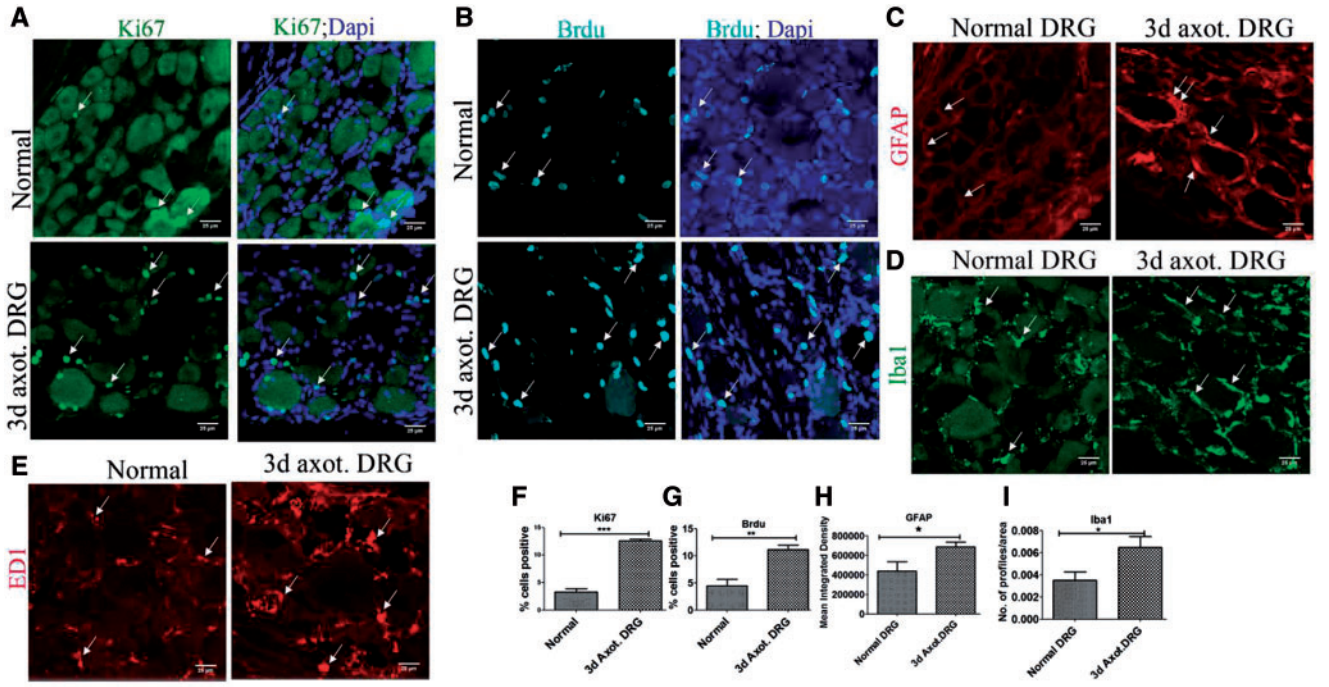

FIGURE 1. DRCCs in normal and injured DRG. **(A)** Expression of Ki67 (arrows) in normal and axotomized DRGs indicates proliferation of resident cells in the DRGs. **(B)** Brdu incorporation (arrows) in normal and axotomized DRGs indicates generation of new cells in the DRGs. **(C)** GFAP expression (arrows) shows increased activation/turnover of SGCs in axotomized DRGs. **(D)** Iba1$^+$ macrophages(arrows) increased accumulation in axotomized DRGs. **(E)** ED1$^+$ macrophages (arrows) increased accumulation in axotomized DRGs. **(F–I)** Quantification of **(A, B, C, D)** showing increased expression of ki67, Brdu, GFAP, and Iba1, respectively, in 3-day axotomized DRGs. Ki67$^+$ cell number is expressed as the percentage of total number of DAPI$^+$ cells, $n = 3$ animals for each group, number of cells, 2681 for normal, 1786 for axotomized DRG, $p = 0.0001$, $df = 4$, $^{***}p < 0.05$ (Student *t*-test, two-tailed). Brdu$^+$ cell number is expressed as the percentage of total number of DAPI$^+$ cells, $n = 3$ animals for each group, number of cells, 2142 for normal, 2202 for axotomized DRG, $p = 0.0098$, $df = 4$, $^{**}p < 0.05$ (Student *t*-test, two-tailed). GFAP levels are expressed as mean integrated intensity calculated using Image J after subtracting background signals in a total field area of 52355.3 μm^2, $n = 3$/group, $p = 0.0395$, $df = 4$, $^{*}p < 0.05$ (Student *t*-test, one-tailed). Iba1 profiles were measured using Image J threshold method and expressed as number of profiles/area, $n = 3$/group, $p = 0.040$, $df = 4$, $^{*}p < 0.05$ (Student *t*-test, one-tailed). Scale bar: 25 μm.

DRCC populations in adult DRGs include both SGCs and macrophages. DRG resident macrophage proliferation was dependent on colony stimulating factor 1 receptor (CSF1R). We also found a potential facilitatory role for the resident macrophages on the spatial organization of SGCs in the DRG. Taken together, our results show interesting local turnover of both SGCs and macrophages in the DRG that is accelerated post-axotomy, and a direct but not well-characterized functional role for macrophages on collaborating with repopulating SGCs.

MATERIALS AND METHODS

Sciatic Nerve (SN) Transection Injury

The sciatic nerve transection was carried out in male adult SD rats (4–6 weeks old) weighing 140–170 g. The protocols were reviewed and approved by the animal care committee at the University of Alberta. Briefly, a small incision was made at the mid-thigh level of anesthetized animals. With the help of sharp scissors, the underlying muscle tissue was separated to expose the SN and a complete transection of the nerve was made at the mid-thigh level. Immediately after the transection, the muscle and skin tissues were sutured back. The animals were given buprenorphine twice daily. The third day following the transection, the animals were euthanized and L4 and L5 DRGs were harvested for immunohistochemistry. For time-dependent analysis, the DRGs were harvested at defined time intervals following SN transection.

Immunohistochemistry

The DRGs were fixed in Zamponi's solution for overnight at 4°C, then washed thrice in PBS and cryoprotected using 20% sucrose for 24 hours at 4°C. After 3 PBS washes, the tissues were embedded on OCT compound. Twelve-micrometer-thick sections of the DRGS were made and the sections were blocked using 5% donkey serum containing 0.3% TritonX100.The primary antibodies used were Ki67 (rabbit, Thermo Fisher Scientific, Waltham, MA; mouse, BD Pharmingen, Franklin Lakes, NJ), Iba1 (rabbit, Wako Chemicals, Richmond, VA; mouse, EMD Millipore, Burlington, MA), ED1 (mouse, EMD Millipore), GFAP (mouse, Sigma

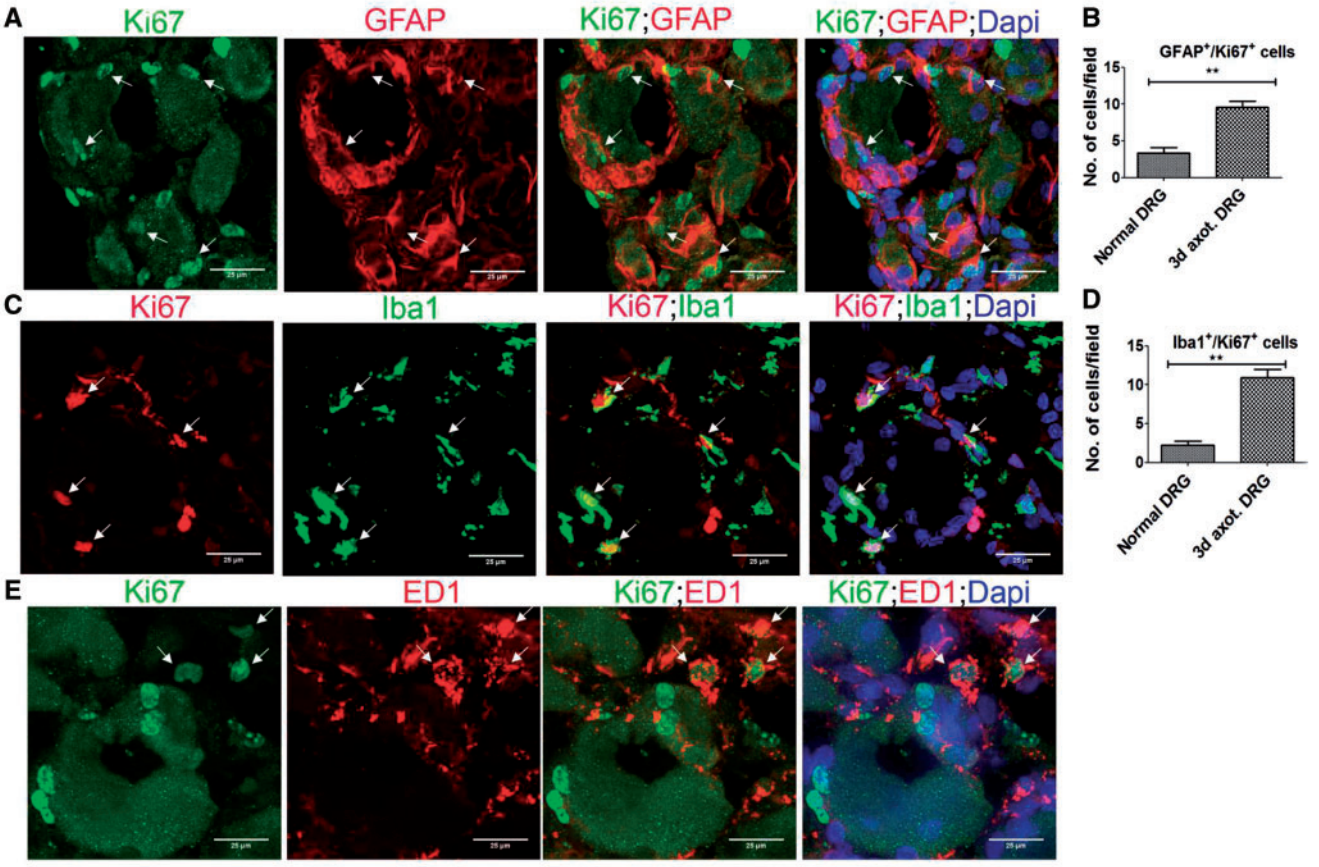

FIGURE 2. Proliferation of SGCs and macrophages in axotomized DRG. **(A, C, E)** Co-expression of Ki67 and GFAP **(A)**, Iba1 **(C)** or ED1 **(E)** indicates local proliferation of SGCs **(A)** and macrophages **(C, E)** in 3-day axotomized DRGs ($Ki67^+$ cells expressing GFAP, Iba1 or ED1 are shown using arrows). Scale bar: 25 μm. **(B)** Quantification of **(A)** shows increased proliferation of SGCs in axotomized DRGs. The quantification was done using Image J software by counting the number of $GFAP^+/Ki67^+$cells in multiple fields of 52355.3 μm^2 area in a given sample, n = 3/group, p = 0.0051, df = 4, **$p < 0.05$ (Student *t*-test, two-tailed). **(D)** Quantification of **(C)** shows increased proliferation of $Iba1^+$ macrophages in axotomized DRGs. The quantification was done using Image J software by counting the number of $Iba1^+/Ki67^+$cells in multiple fields of 52355.3 μm^2 area in a given sample, n = 3/group, p = 0.0017, df = 4, **$p < 0.05$ (Student *t*-test, two-tailed).

Aldrich; Rabbit, Sigma Aldrich), Sox2 (goat, R&D Systems, Minneapolis, MN; mouse, Abcam, Cambridge, UK; rabbit, Abcam), CSF1R (rabbit, Sigma Aldrich, St. Louis, MO) and NeuN (mouse, EMD Millipore). The primary antibodies were incubated for 1 hour at room temperature (RT), followed by secondary antibodies for 1 hour at RT. The secondary antibodies used were antimouse cy3 (Sigma-Aldrich), antirabbit Alexa Fluor 488 (Life Technologies, Carlsbad, CA), antirabbit Alexa Fluor 546 (Life Technologies), antimouse Alexa Fluor 633 (Life Technologies), antimouse Alexa Fluor 488 (Life Technologies), and antigoat Alexa Fluor 546 (Life Technologies). Experiments without primary antibodies were performed for each secondary antibody used in the study to verify absence of nonspecific signals. The sections were mounted using Vectashield mounting media containing DAPI (Vector Laboratories, Burlingame, CA). All the images were captured using a confocal microscope, WaveFX, Olympus. The images were analyzed using Image J Fiji software.

Brdu Incorporation Assay

Brdu (Sigma-Aldrich) was dissolved in 1 mM Tris, 0.8% NaCl, 0.25 mM EDTA solution and 25 mg/2 mL was administered intraperitoneally (ip) to SD rats 1 hour prior to SN transection, followed by daily ip administration for another 3 days. The DRGs were harvested on the third day following transection. For detection of Brdu incorporation, the DRG sections were incubated with 2 N HCl for 30 minutes, washed 3 times in PBS then dipped in 0.01% trypsin at 37°C for 3 minutes. Next, the sections were washed thrice in PBS and blocked using 5% donkey serum containing 0.3% triton X100. The sections were then incubated with Brdu antibody (mouse monoclonal, Sigma Aldrich, or rabbit polyclonal, Thermo Fisher Scientific, or chicken polyclonal, Abcam) for 1 hour at RT, followed by the corresponding secondary antibody for 1 hour at RT (antimouse cy3, Sigma Aldrich, or antirabbit Alexa Fluor 488, Life Technologies, or antichicken Alexa Fluor 546, Invitrogen, Carlsbad, CA). The sections were mounted using Vectashield mounting medium containing

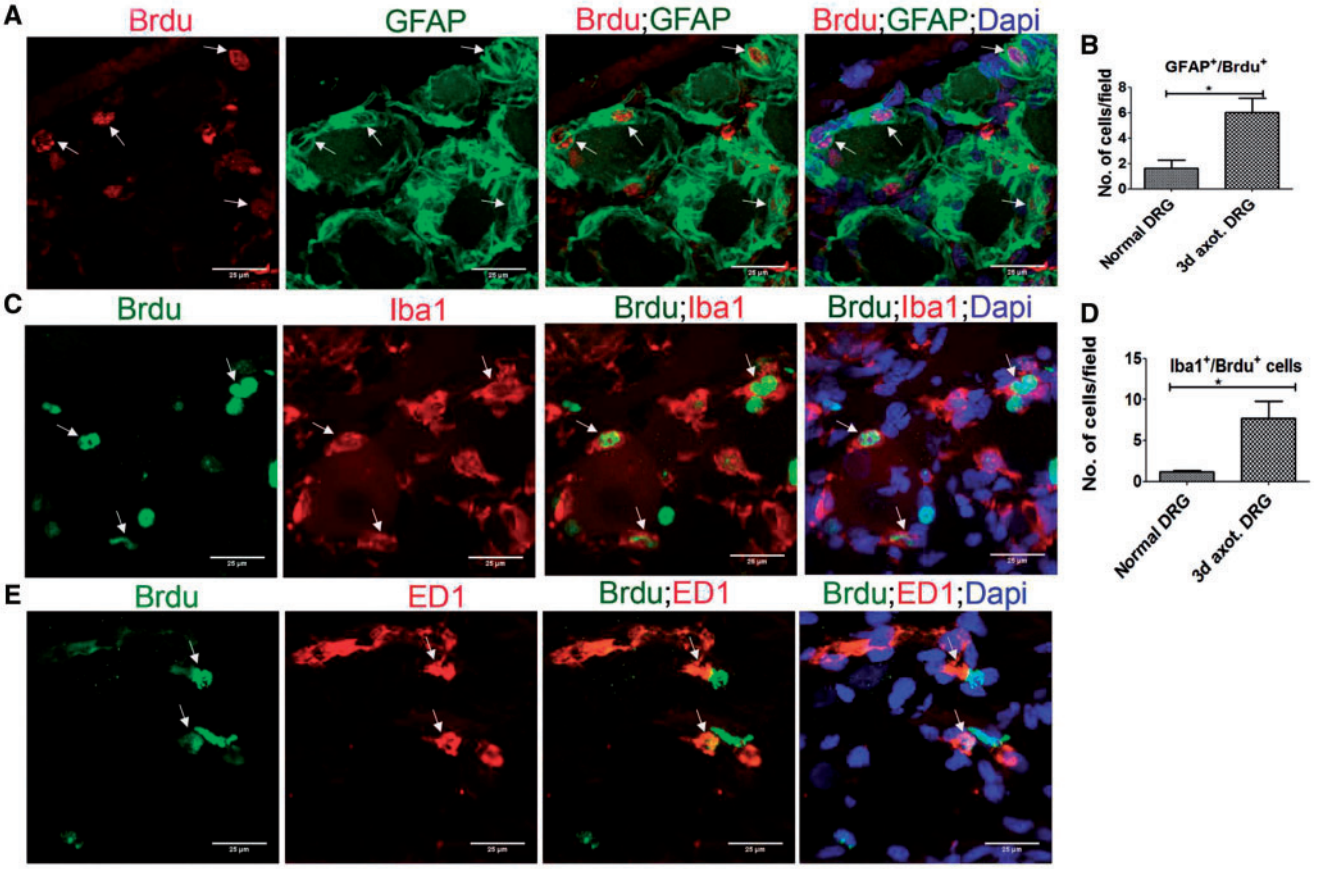

FIGURE 3. Newborn SGCs and macrophages in axotomized DRG. **(A, C, E)** Brdu incorporation in GFAP+ **(A)**, Iba1+ **(C)** or ED1+ **(E)** cells shows generation of SGCs and macrophages in axotomized DRGs (Brdu+ cells expressing GFAP, Iba1 or ED1 are shown using arrows). Scale bar: 25 μm. **(B)** Quantification of **(A)** shows increased proliferation of SGCs in axotomized DRGs. The quantification was done using Image J software by counting the number of $GFAP^+/Brdu^+$ cells in multiple fields of 52355.3 μm^2 area in a given sample, n = 2/control, n = 3/axotomized group, p = 0.0314, df = 3, **p < 0.05 (Student *t*-test, one-tailed). **(D)** Quantification of **(C)** shows increased proliferation of $Iba1^+$ macrophages in axotomized DRGs. The quantification was done using Image J software by counting the number of $Iba1^+/Brdu^+$ cells in multiple fields of 52355.3 μm^2 area in a given sample, n = 2/group, p = 0.0451, df = 2, *p < 0.05 (Student *t*-test, one-tailed).

DAPI. Confocal images were taken using WaveFX, Olympus, and the images were analyzed using Image J Fiji software.

Coculture of DRG Cells

For coculture of injured sensory neurons, SGCs and macrophages, L4-L6 DRGs were harvested from SN transected animals as described above. Individual neurons were dissociated as described previously (13). Briefly, the pooled DRGs were incubated in 0.1% collagenase (Sigma-Aldrich) for 90 minutes at 37°C. Individual neurons and perineuronal cells were then mechanically dissociated, using repeated pipetting, centrifuged and collected in a pellet. The pellet was then washed in L15 media (invitrogen) twice and then overlaid on 15% BSA solution and centrifuged at 800 rpm for 6 minutes to separate perineuronal cells from neurons. The pelleted neurons were washed in L15 and seeded on to Poly-L-lysine (PLL) and laminin-coated 4-well chambered slides. The culture media contained DMEM/F12 (Gibco, Waltham, MA), N2 supplement (1:100; Gibco), NGF (100 ng/mL; Life Technologies) and penicillin and streptomycin (50 U/mL; Gibco). The perineuronal cell fraction, which contains SGCs and macrophages, was then centrifuged, washed in L15 and then seeded with neurons in the culture wells.

Clodronate-Liposomes Treatment

The clodronate liposome experiments were carried out in SN transected adult CD1 mice weighing 20–25 g. 150 μl of the codronate liposome suspension (7 mg/mL; FormuMax scientific) was given ip twice, one day before and 2 days after SN transection. The DRGs were harvested on the third day after the transection.

Flow Cytometry of Peripheral Blood Cells

White blood cells were isolated from whole blood collected from mouse treated or untreated with clodronate-liposomes. These cells were then prepared for fluorescence-activated cell sorting (FACS) flow cytometry. Cell pellets

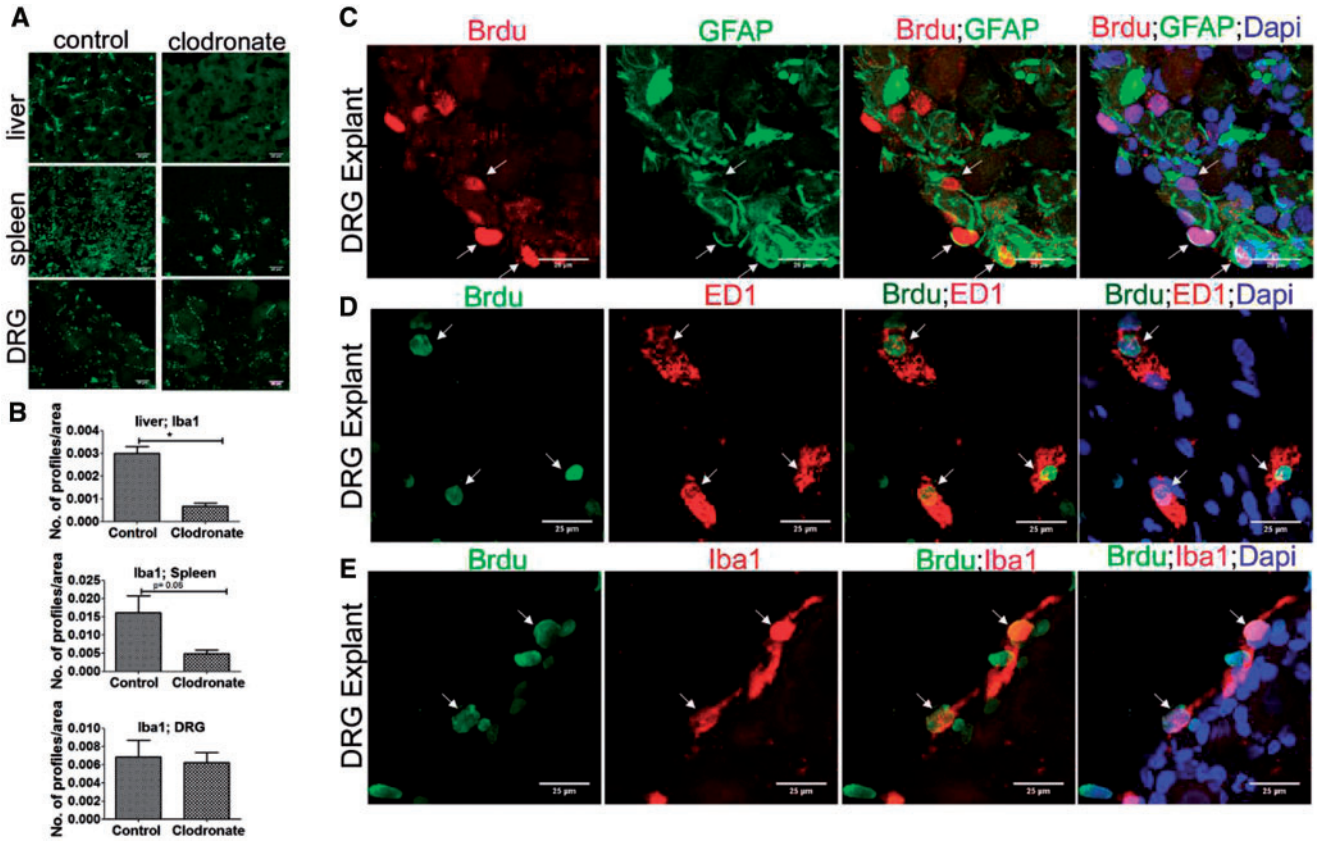

FIGURE 4. Blood monocytes deprivation has no effect on proliferation of resident macrophages and SGCs in DRG. **(A)** Clodronate-liposome treatment completely or partially depletes macrophages (green; Iba1$^+$) in liver and spleen respectively, but not DRG. Scale bar: 25 μm. **(B)** Quantification of **(A)** shows depletion of Iba1$^+$ macrophages in the liver and spleen, but not DRG, after clodronate treatment. Iba1$^+$ profiles were measured using Image J threshold method and expressed as number of profiles/area, n = 2/group. For liver, p = 0.0209, df = 2, *p < 0.05 (Student *t*-test, two-tailed); spleen, p = 0.0698, df = 2 (Student *t*-test, one-tailed), DRG, p = 0.4015, df = 2 (Student *t*-test, one-tailed). **(C)** Brdu uptake in GFAP$^+$ cells in the DRG explant indicates local turnover of SGCs. **(D)** Brdu uptake in ED1$^+$ cells in the DRG explant indicates local turnover of macrophages. **(E)** Brdu uptake in Iba1$^+$ cells in the DRG explant indicates local turnover of macrophages. (Brdu$^+$ cells expressing GFAP, ED1 or Iba1 are shown using arrows). Scale bar: 25 μm.

were resuspended in the FACS buffer, which consisted of PBS supplemented with 10% heat-inactivated fetal bovine serum (FBS). The final concentration of each cell suspension was adjusted to 1×10^6 cells/mL in ice-cold FACS buffer and transferred to Falcon round bottom polystyrene tubes. Cells were washed twice in cold PBS and then centrifuged at 200*g* for 5 minutes and the supernatant was discarded. The cells were then pelleted for 5 minutes at 1100*g* and resuspended in 100 μl of Mouse BD Fc Block (BD Biosciences, Mississauga, Ontario) (diluted 1:50 in FACS buffer) and incubated for 30 minutes on ice to avoid any nonspecific binding and background fluorescence. Each sample of cells were stained with LY-6G antibody (BD Biosciences), by adding an appropriate volume as per manufacturer's protocol. Cells were incubated for 30 minutes in the dark on ice. Following incubation, cells were washed 3 times by centrifugation at 525*g* for 5 minutes and resuspended in 400 μl of ice-cold FACS buffer and stored at 4°C in the refrigerator until analysis. Compensation tubes (BD Biosciences) were used to distinguish each fluorochrome and to avoid any spectral overlap. Compensation beads were stained as described above for staining cells.

Data were acquired by running the samples on the BD FACSCanto II (BD Biosciences) with 10 000 events collected for each tube. The data were analyzed using BD FACSDiva software (BD Biosciences). First the cells were gated using the forward scatter (FSC) and side scatter (SSC) to find viable, single cell events. Gating excluded events with low FSC and high SSC. Using a histogram, 2 different populations of cells were analyzed: positive and negative for LY-6G. The percent of each cell population queried was automatically generated by the software in the histogram and was compared among the samples.

DRG Explant Culture

The DRGs were harvested from adult SD rats at 24 hours to 3 days postSN transection. The whole DRGs were then seeded on 4 well chamber slides precoated with PLL, laminin and heat inactivated FBS. During the first 4–6 hours,

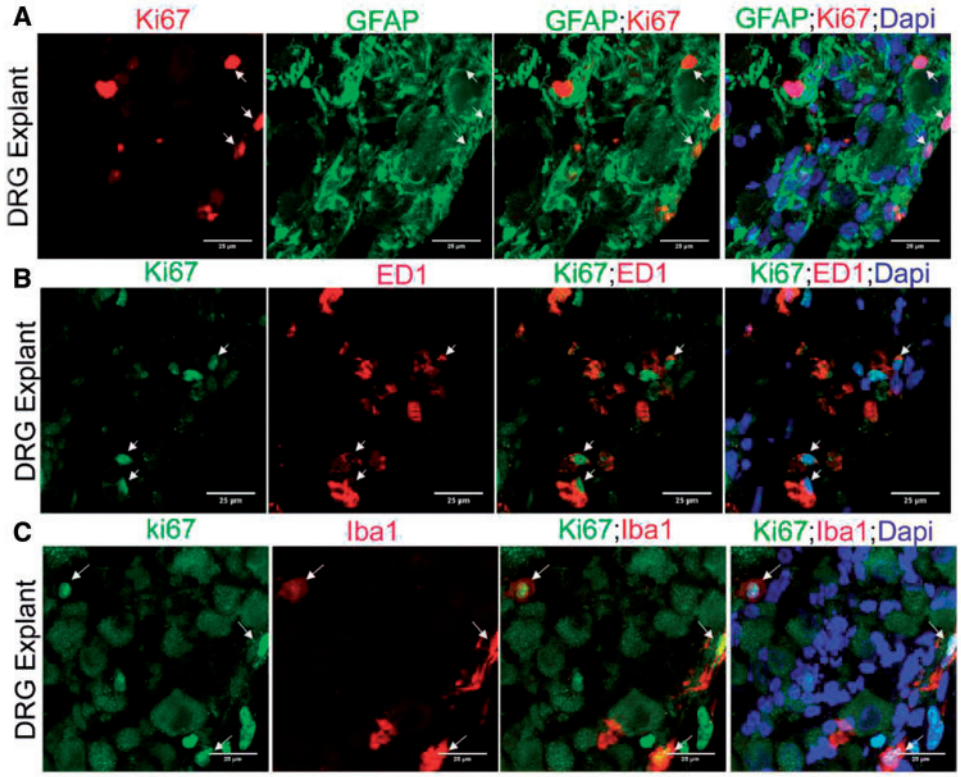

FIGURE 5. Local turnover of macrophages and SGCs in DRG explant culture. **(A)** Ki67 expression in GFAP$^+$ cells in the DRG explant indicates local turnover of SGCs. **(B)** Ki67 expression in ED1$^+$ cells in the DRG explant indicates local turnover of macrophages. **(C)** Ki67 expression in Iba1$^+$ cells in the DRG explant indicates local turnover of macrophages. (Ki67$^+$ cells expressing GFAP, ED1 or Iba1 are shown using arrows). Scale bar: 25 μm.

the DRGs were maintained in 200 μl of FBS and then on DMEM/F12 (Gibco) containing N2 supplement (1:100; Gibco), NGF (100 ng/mL; Life Technologies), penicillin and streptomycin (50 U/mL; Gibco), and 10%FBS. The medium also contained 20 μM Brdu. The DRG explants were maintained for 5–7 days in culture before performing immunohistochemistry.

For the CSF1R inhibition assay, the DRG explant culture was incubated with BLZ945 (Cayman Chemicals, Ann Arbor, MI) at different concentrations ranging from 50 to 200 nM from the second to fifth day of the culture. Quantification of macrophages proliferation was done by manual counting of Brdu$^+$/ED1$^+$ cells at different fields from untreated and treated DRGs.

Tunel Assay

Tunel assay was performed using the ApopTag Plus Fluorescein InSitu Apoptosis Detection kit from EMD Millipore, according to the manufacturer's protocol.

Experimental Design and Statistical Analysis

For quantification of Ki67$^+$, Brdu$^+$ and Sox2$^+$ cells, 3 animals were considered for each group. L4 DRG from each animal was used and images were captured from different fields for quantification. Results were calculated as means ± SEM. A Student *t*-test or ANOVA was used to identify statistical significance. Significance was set at $p \leq 0.05$. More specific details on quantification, statistical approaches and number of cells considered are described under respective figure legends. Size of the scale bar for each image is mentioned in the figure legends separately.

RESULTS

DRCCs in the Normal and Injured Adult DRG

We evaluated DRCCs in normal and 3-day axotomized rat DRGs based on both Ki67 expression and incorporation of Brdu. Unexpectedly, Ki67$^+$ and Brdu$^+$ cells were identified in the normal uninjured DRG indicating an unappreciated level of ongoing cell division in apparently stable ganglia. However, there was a striking rise in the number of DRCCs after axotomy (Fig. 1A, B, F, G).

To reveal the precise identity of DRCCs, we first evaluated which population of cells expands in the DRG after axotomy. GFAP, a previously well-known marker for SGCs, was used to mark SGCs in our study (14). We found rises in GFAP$^+$ cells in the axotomized DRG indicating activation and potential turnover of SGCs. Several large caliber neurons had remarkable focal expansion of activated SGCs surrounding them indicating repopulation of SGCs around injured neurons (Fig. 1C, H).

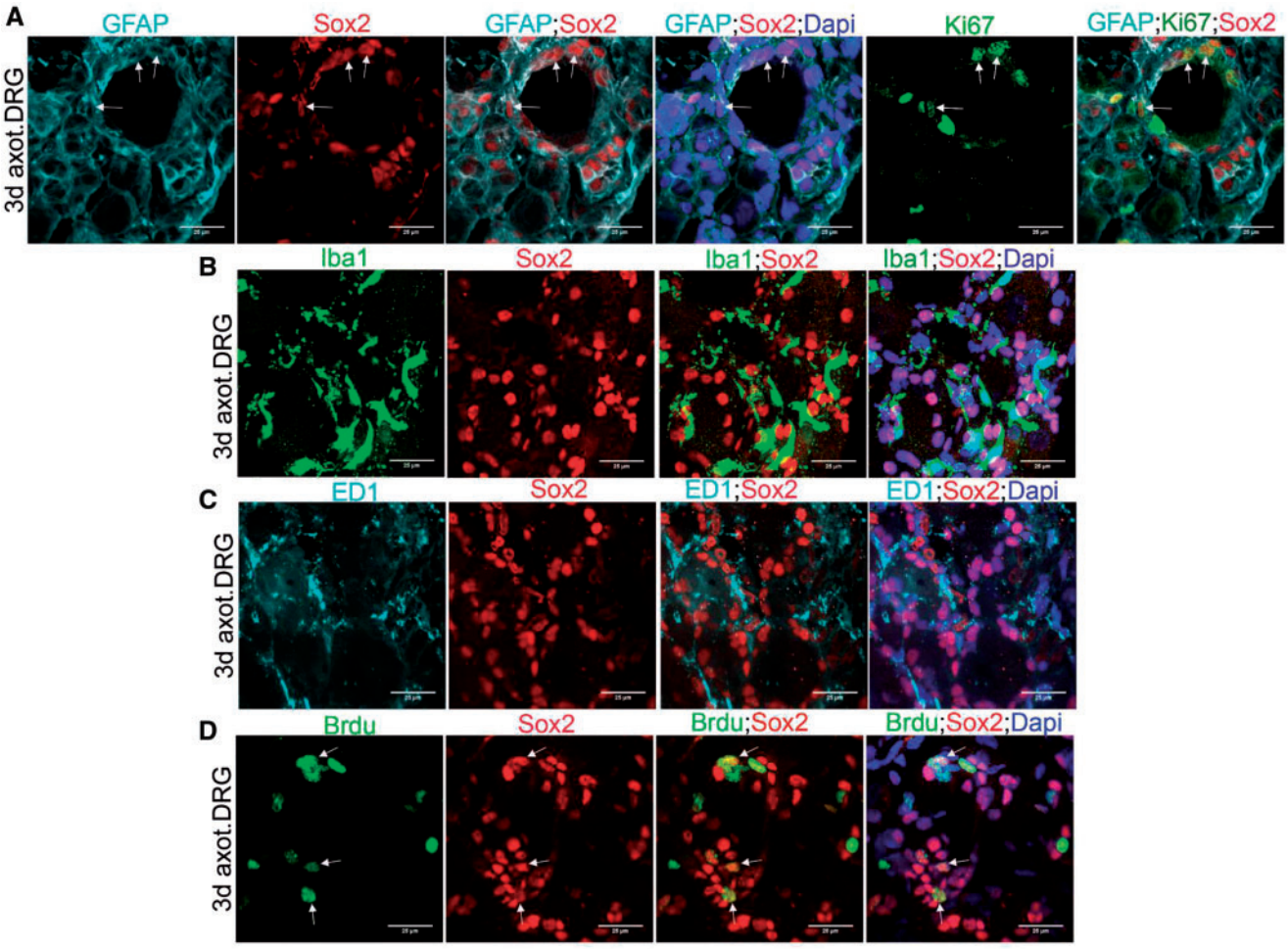

FIGURE 6. SGCs selectively express Sox2 in DRG. **(A)** Co-expression of Sox2 and GFAP in 3-day axotomized DRG shows $Sox2^+$ SGCs. The $Ki67^+$SGCs also express Sox2 ($GFAP^+/Ki67^+/Sox2^+$ cells are shown using arrows). **(B)** Expression of Sox2 and Iba1 in 3-day axotomized DRG shows lack of Sox2 expression in $Iba1^+$ macrophages. **(C)** Expression of Sox2 and ED1in 3-day axotomized DRG shows lack of Sox2 expression in $ED1^+$ macrophages. **(D)** Co-expression of Sox2 and Brdu in 3-day axotomized DRG shows cycling $Sox2^+$ cells ($Brdu^+/Sox2^+$ cells are shown using arrows). Scale bar: 25 μm.

Macrophages express both Iba1 and ED1 (15). Although it might be assumed that Iba1 and ED1 identify similar populations of macrophages, in the DRG we noted that while an overlapping population existed, they also marked distinct populations (Supplementary Data Fig. S1A). The number of both $Iba1^+$ and $ED1^+$ macrophages appeared to increase in the axotomized DRGs (Fig. 1D, E). The increase in turnover of Iba1 macrophages was later quantified and confirmed (Fig. 1I). Overall our results indicate that local expansion of SGCs and macrophages occurs in adult DRG after axotomy.

Proliferation of SGCs and Macrophages in Adult Uninjured DRG

We double-labeled DRG with Ki67 and GFAP, Iba1, ED1 or NeuN to characterize DRCCs in adult uninjured DRG (Supplementary Data Fig. S2). A small population of cells with a modest rise in GFAP expressed Ki67 indicating basal expansion of SGCs in the absence of injury. Similarly, we observed proliferation of macrophages evidenced by their combined expression of Ki67 and Iba1 or ED1 within uninjured DRGs. Double labeling of DRG with Brdu and GFAP, Iba1or ED1 also showed newborn SGCs and macrophages in the DRG, generated within the 4 days of Brdu administration (Supplementary Data Fig. S3). There were no $Ki67^+$ or $Brdu^+$ neurons present. The findings overall indicate that SGCs and macrophages locally turnover in the normal uninjured DRG.

Axotomy-Induced DRCC Expansion Involves SGCs and Macrophages

We next identified that the remarkable expansion of DRCCs after axotomy involves both SGCs and macrophages. Most of the proliferating $Ki67^+/GFAP^+$ SGCs and $Ki67^+/Iba1^+$ macrophages were localized around neurons (Fig. 2A, C). However proliferating $Ki67^+/ED1^+$ macrophages appeared at random locations in the DRG (Fig. 2E).

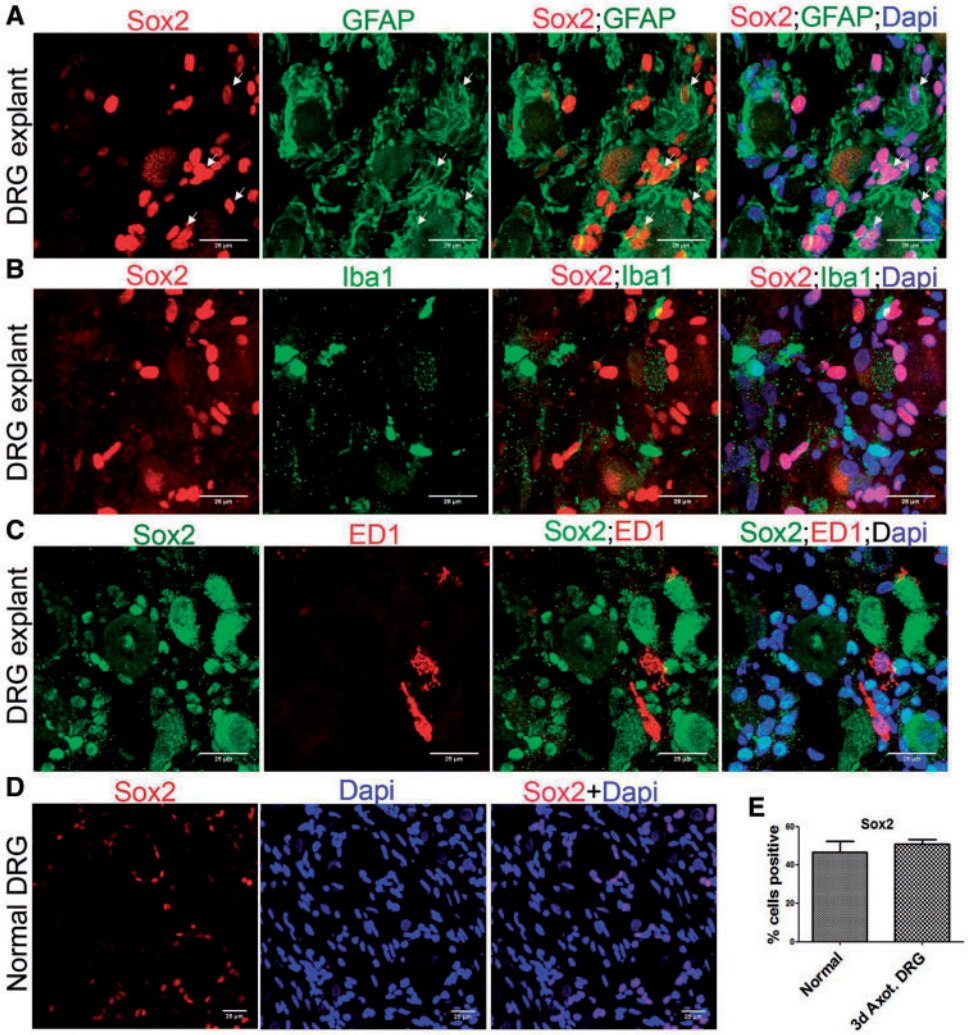

FIGURE 7. SGCs selectively express Sox2 in DRG explants. **(A)** Co-expression of Sox2 and GFAP in DRG explant shows $Sox2^+$ SGCs ($GFAP^+/Sox2^+$ cells are shown using arrows). **(B)** Expression of Sox2 and Iba1 in DRG explant shows lack of Sox2 expression in $Iba1^+$ macrophages. **(C)** Expression of Sox2 and ED1 in DRG explant shows lack of Sox2 expression in $ED1^+$ macrophages. **(D)** $Sox2^+$ cells are present in adult uninjured DRG. **(E)** Quantification of number of $Sox2^+$ cells in normal and 3-day axotomized DRGs shows no significant difference. The number of $Sox2^+$ cells is expressed as the percentage of total number of $DAPI^+$ cells, n = 3 animals for each group, number of cells, 1491 for normal, 1915 for axotomized DRG, no statistical significance (Student *t*-test, two-tailed). Scale bar: 25 μm.

We quantified $GFAP^+/Ki67^+$ or $Iba1^+/Ki67^+$ double-positive cells and found a significant rise in proliferating SGCs and macrophages in the axotomized DRGs (Fig. 2B, D). None of the $Ki67^+$ cells was $NeuN^+$, excluding neuronal division (Supplementary Data Fig. S4A). Brdu uptake assay further confirmed the proliferation of SGCs and macrophages in axotomized DRGs, whereas no neurons were positive for Brdu indicating the absence of neurogenesis (Fig. 3; Supplementary Data Fig. S4B). The newly generated $Brdu^+$ SGCs and $Iba1^+$ macrophages were largely located around injured neurons whereas $Brdu^+/ED1^+$ macrophages were randomly distributed in the DRG. A preliminary time-dependent assessment of the proliferation kinetics of $Ki67^+/ED1^+$ macrophages further revealed a trend for increased proliferation of macrophages at the onset of 48 hours postaxotomy, which peaked at 72 hours and then declined from 7 days onwards (Supplementary Data Fig. S4C).

Blood Monocytes Deprivation Has No Effect on Repopulation of Resident Macrophages and SGCs in Adult DRG

Infiltration of blood monocytes are the main source of macrophages in peripheral tissues. To eliminate the interference of infiltrating monocytes in our study, we treated mice with clodronate-liposomes and depleted blood monocytes. Ly6G, which is a common marker for monocytes and neutrophils, was used to confirm monocyte depletion. Our FACS analysis showed a reduction of $Ly6G^+$ cells after clodronate-liposomes treatment confirming successful

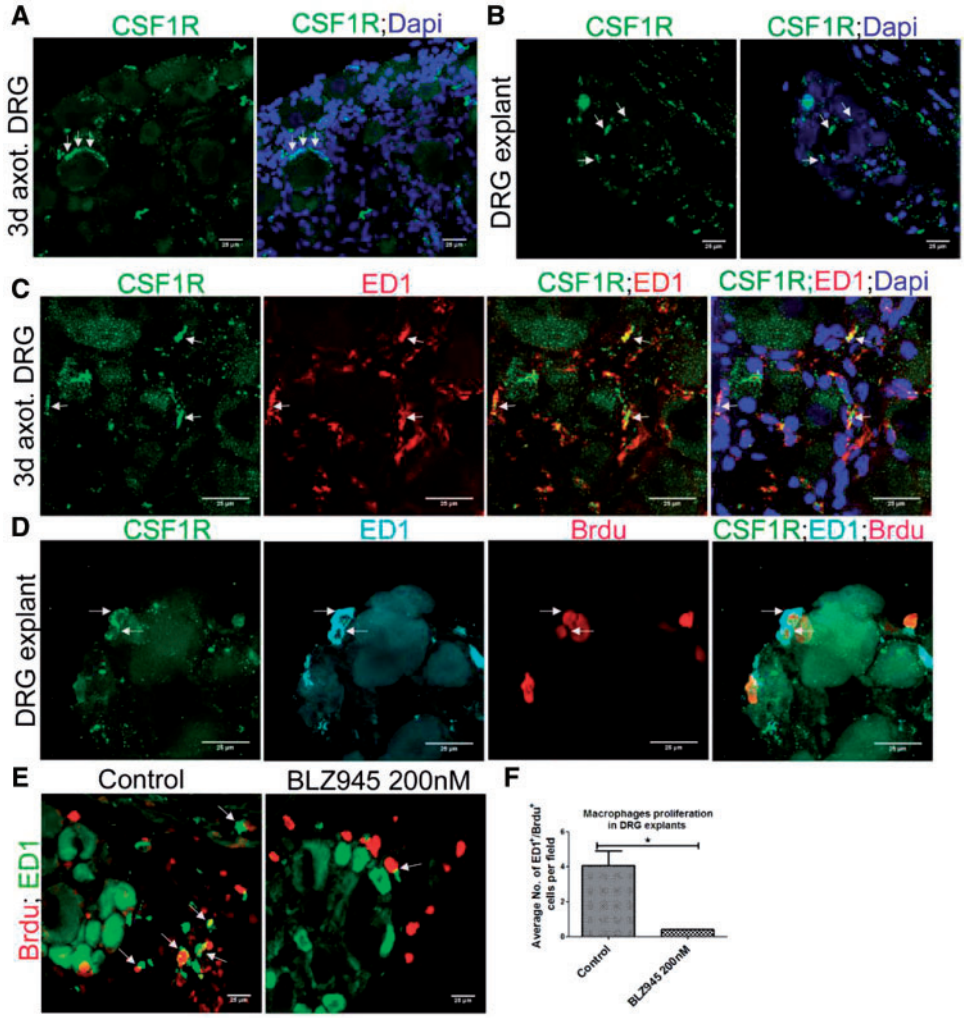

FIGURE 8. Proliferation of DRG resident macrophages is CSF1R-dependent. **(A)** CSF1R is expressed in 3-day axotomized DRG (arrows). Scale bar: 25 μm. **(B)** CSF1R is expressed in a DRG explant in vitro (arrows). Scale bar: 25 μm. **(C)** $ED1^+$ macrophages express CSF1R ($CSF1R^+/ED1^+$ macrophages are shown using arrows). Scale bar: 25 μm. **(D)** Brdu incorporation in $ED1^+/CSF1R^+$ macrophages shows proliferation of $ED1^+/CSF1R^+$ macrophages ($CSF1R^+/ED1^+/Brdu^+$ cells are shown using arrows). Scale bar: 25 μm. **(E)** Reduction in $ED1^+/Brdu^+$ macrophages in DRG explant culture after BLZ945 treatment ($ED1^+/Brdu^+$ macrophages are shown using arrows). Scale bar: 25 μm. **(F)** Quantification of **(E)**, n = 3/group, p = 0.0116, df = 4, *$p < 0.05$ (Student *t*-test, two-tailed).

depletion of monocytes (Supplementary Data Fig. S4D). We also found a complete and partial depletion of macrophages in the liver and spleen respectively after monocyte depletion (Fig. 4A, B). However, there was no reduction in macrophages abundance in the DRG after clodronate treatment (Fig. 4A, B). Our findings thus provide remarkable evidence that macrophages can repopulate in axotomized DRG without significant contribution from blood-borne monocytes.

Previous studies indicated that DRG blood ganglion barrier may prevent the entry of clodronate-liposomes to DRGs explaining why resident macrophages was not directly targeted in our study.

We next studied DRCCs in DRG explant culture to confirm the strict local origin of resident macrophages and SGCs. Through this approach we completely eliminated the possibility of infiltrating monocytes in our study. DRGs were isolated at different time intervals after axotomy, ranging from 24 hours to 3 days, and the whole DRG culture was performed for 5–7 days in vitro in the presence of Brdu. Interestingly, at all conditions the resident macrophages and SGCs did proliferate, evidenced by both Brdu incorporation and Ki67 expression (Figs. 4C–E, 5). This result further confirms our findings that resident macrophages and SGCs are mitotic in the axotomized DRG milieu.

SGCs Selectively Express Sox2

Sox2 is a stem cell marker expressed in dedifferentiated cells. Sox2 participates in Schwann cell sorting in the

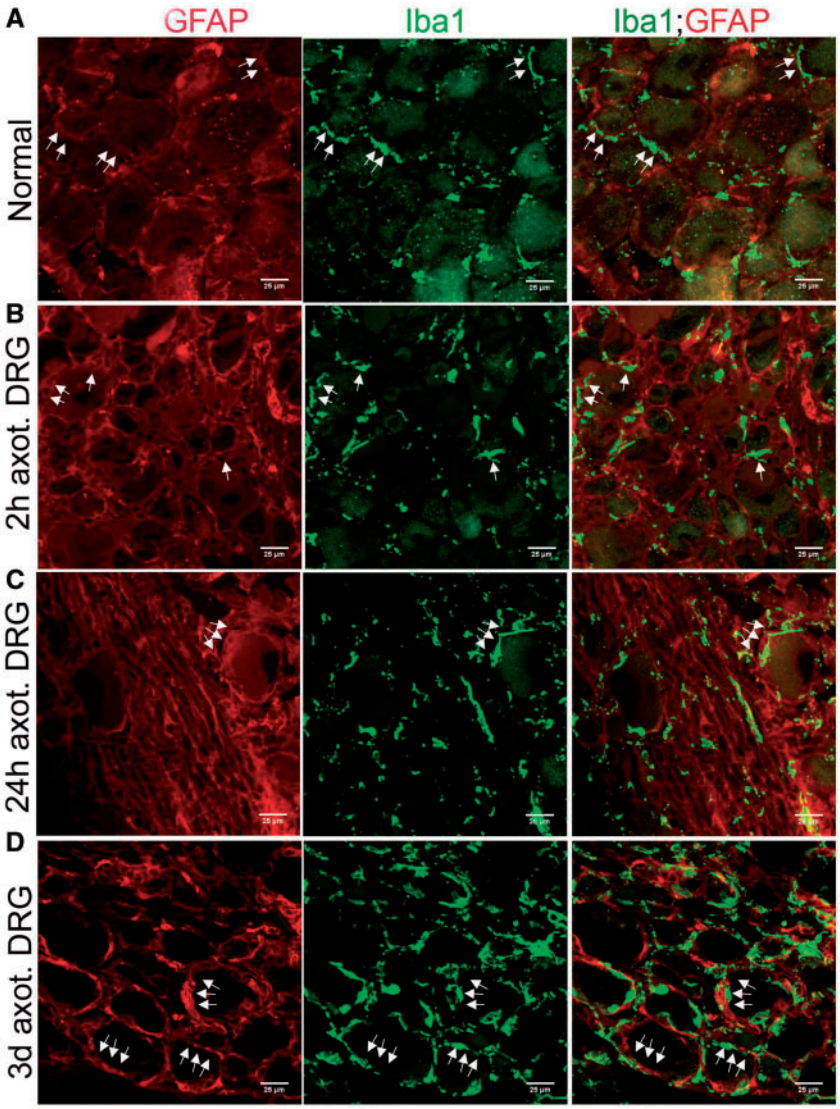

FIGURE 9. Macrophages physically interact with SGCs in DRG. **(A, B)** Iba1$^+$ macrophages occupy overlapping locations of GFAP$^+$ SGCs in uninjured and 2-hour postaxotomized DRGs (arrows). **(C)** Iba1$^+$ macrophages in 24-hour postaxotomized DRG elongate processes and spatially align with early activated GFAP$^+$ SGCs (arrows). **(D)** Iba1$^+$ macrophages in 3-day axotomized DRG spatially align with fully activated GFAP$^+$ SGCs (arrows). Scale bar: 25 μm.

peripheral nerves (16). We assessed the expression of Sox2 in axotomized DRG to evaluate whether it might specifically label DRCCs. Interestingly, Sox2 was present in GFAP$^+$ SGCs but not in either Iba1$^+$ or ED1$^+$ macrophages, suggesting distinct molecular machineries in SGCs and macrophages during their individual turnover (Fig. 6A–C). We also assessed the cycling potential of Sox2$^+$ SGCs by colabeling the cells with Sox2, GFAP and Ki67 and found that Sox2$^+$ SGCs proliferate locally (Fig. 6A). Sox2$^+$ cells also took Brdu confirming their doubling potential (Fig. 6D). Interestingly macrophages were found in close proximity to Sox2$^+$ cells (Fig. 6B, C). Given the well-known role for Sox2 on cell sorting, the proximal presence of macrophages to Sox2$^+$ cells may potentially favor a macrophages-assisted sorting of Sox2$^+$ SGCs in axotomized DRGs.

The SGC specific expression of Sox2 was also apparent in our DRG explant model (Fig. 7A–C). We found that adult uninjured DRG also express Sox2$^+$ cells similar in frequency to axotomized DRGs (Fig. 7D, E). This suggests an ongoing physiological role for Sox2, potentially involved with spatial and temporal arrangement of SGCs. We noted the presence of a few Sox2$^+$/GFAP$^-$ cells also in the DRG.

Local Proliferation of DRG Resident Macrophages Is CSF1R-Dependent

Colony stimulating factor 1 (CSF1) is a trophic factor for macrophages and CSF1-CSF1R signaling is critical for proliferation of mature macrophages in tissues (17). A recent report showed that DRG neurons secrete CSF1 in response to

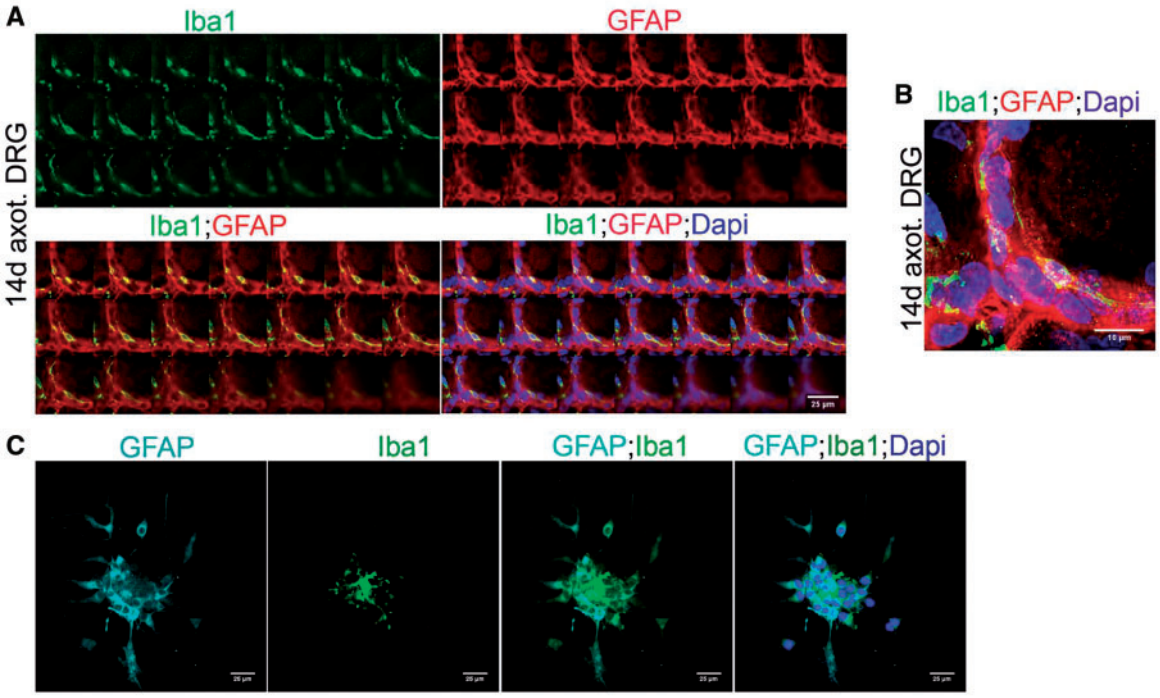

FIGURE 10. Macrophages physically interact with SGCs in axotomized DRGs in vivo and co culture in vitro. **(A)** Part of the "Z" stack images of a 14-day axotomized DRG shows spatial alignment of Iba1$^+$ macrophages with GFAP$^+$ SGCs. Scale bar: 25 μm. **(B)** Maximum intensity projection of the Z stack images in **(A)**. Scale bar: 10 μm. **(C)** Coculture of axotomized DRG neurons, macrophages and SGCs shows Iba1$^+$ macrophages apparently sequestrating an SGC (GFAP$^+$) cluster. Scale bar: 25 μm.

distal axotomy. Therefore, we examined whether CSF1 signaling is involved in the cycling of DRG resident macrophages. Strikingly, we found CSF1R expression in both axotomized DRGs in vivo and DRG explants in vitro (Fig. 8A, B). Further, we confirmed CSF1R expression in ED1$^+$ macrophages in axotomized DRG (Fig. 8C). In addition, Brdu uptake by CSF1R$^+$/ED1$^+$ macrophages revealed that CSF1R$^+$ macrophages proliferate (Fig. 8D). To further confirm the role of CSF1R signaling on DRG resident macrophage division, we treated DRG explant cultures with a selective inhibitor for CSF1R, BLZ945 (17), and this inhibited macrophages proliferation and confirmed that the proliferation of DRG resident macrophages is CSF1R-dependent (Fig. 8E, F).

Elongated Processes of Macrophages Align With the Spatial Arrangement of SGCs

To investigate a functional role for macrophages in DRG, we first asked whether they have any apparent regulatory role over SGC activation. In order to address this, we examined the time course of macrophages accumulation and SGC activation in axotomized DRGs. As noted previously, Iba1$^+$ macrophages were present in uninjured, and axotomized DRGs at early intervals of postSN transection, when SGC activation was minimal indicating that macrophages accumulation precedes SGC activation (Fig. 9A, B). These macrophages were distributed at locations overlapping with that of SGCs indicating potential structural interaction between the 2 cell types. At later hours after axotomy, the macrophages elongated their processes and, with their ramifications, surrounded SGCs indicating physical sequestering of SGCs to the perineuronal space (Fig. 9C). Maximum activation of SGCs was observed 3 days after axotomy and at this time macrophages were fully aligned with the spatial distribution of SGCs in the perineuronal rim and this structural interaction persisted even after 14 days of postSN transection (Figs. 9D, 10A, B). This indeed indicated an influence of macrophages over the spatial arrangement of the newly populated SGCs. Supporting this observation, our in vitro coculture also showed that macrophages physically adhere to a SGC cluster (Fig. 10C). On the other hand, a regulatory influence by SGCs on repopulating resident macrophages may also be possible.

Cellular Expansion in the Adult DRG Is Accompanied by Apoptosis

We then asked whether a cellular homeostasis exists in DRGs following the expansion of cells. Tunel staining revealed less frequent but apparent apoptosis in normal DRG (Fig. 11A). As expected, apoptotic events increased in 7-day axotomized DRGs (Fig. 11B; Supplementary Data Fig. S4E). This increased apoptosis at later intervals of axotomy might maintain the cellular homeostasis in DRG following the earlier major expansion of the cells. Colabeling of early apoptotic cells with ED1 or GFAP revealed that both macrophages and SGCs undergo apoptosis (Fig. 11C, D). Overall our results indicated that the major expansion of SGCs and macrophages in

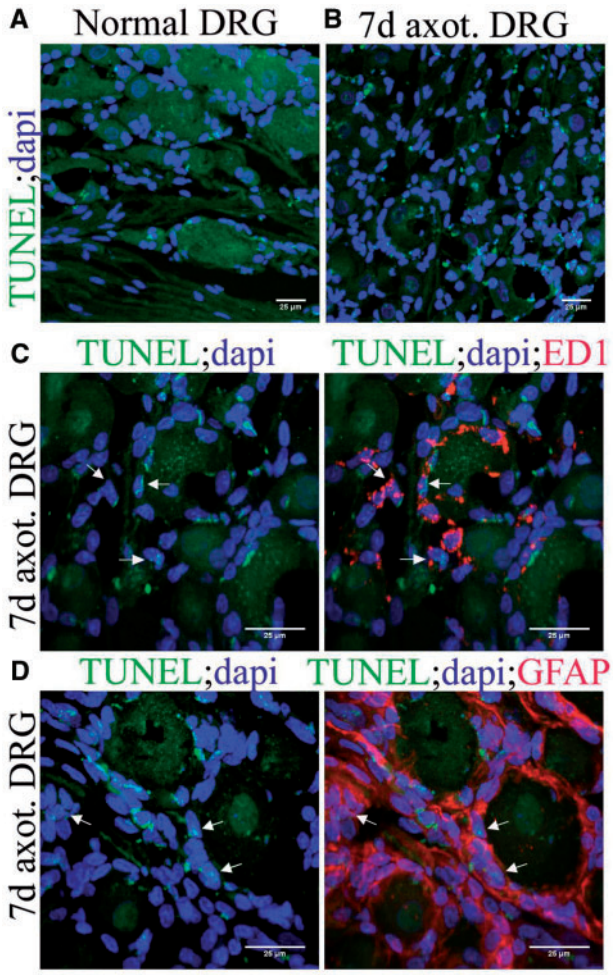

FIGURE 11. Apoptosis in normal and axotomized DRGs. **(A)** Tunel staining in normal DRG. **(B)** Tunel staining revealed increased apoptosis in 7-day axotomized DRG. **(C)** Costaining of ED1 with Tunel revealed that macrophages undergo apoptosis in 7-day axotomized DRG ($TUNEL^+/ED1^+$ cells are shown using arrows). **(D)** Costaining of GFAP with TUNEL revealed that SGCs undergo apoptosis in 7-day axotomized DRG ($TUNEL^+/GFAP^+$ cells are shown using arrows).

the DRG is accompanied by programmed cell death at later intervals.

DISCUSSION

In this study, we identify an active and dynamic DRCC population in DRGs that is dramatically ramped up by a distal axotomy. The apparent impact of axotomy on DRG cellular dynamics far from the injury site is striking. The major findings of this work are: (1) the ongoing presence of a heterogenous population of DRCCs in intact and axotomized DRG, (2) DRG resident macrophages and SGCs form the major subtypes of DRCCs, (3), DRG resident macrophages proliferation is CSF1R-dependent, (4) Sox2 may play a role in SGC dynamics in DRG, and (5) macrophages with their ramified processes structurally interact with SGCs and potentially facilitate spatial organization of SGCs.

While axotomy-induced DRCCs have been recognized, here we show that this involves both macrophages and SGCs, apparently in a form of structural collaboration. It was previously thought that macrophages abundance in axotomized DRGs largely accrues from infiltrating blood monocytes (18). However, our data from Ki67 and Brdu immunolabeling convincingly demonstrate that local cycling also contributes to macrophages expansion in a major way. Clodronate-liposome is a selective approach to deplete blood monocytes without targeting DRG resident macrophages (19). We noted no reduction in DRG resident macrophages in monocyte-depleted animals despite reduction in macrophages in other tissue such as liver and spleen. Thus, it is clear that the macrophages reserve we observed in the DRGs arises from local proliferation of resident macrophages. Our DRG explant model in vitro, that completely eliminates the interference of infiltrating monocytes, also showed rapid expansion of resident macrophages. Overall, our findings reveal an impressive capability of DRG to generate their own inflammatory milieu, a feature that may be applicable to other neuronal systems.

CSF1 offers trophic support to macrophages (17). A recent report showed that DRG neurons secrete CSF1 after peripheral nerve injury (20). We found that DRG resident macrophages express CSF1 receptor. Selective inhibition of CSF1R using the small molecule BLZ945 prevented macrophage expansion in our DRG explant model. BLZ945 is 3200-fold selective to CSF1R compared with other related kinases and has been shown to inhibit bone marrow-derived and tumor-associated macrophages proliferation (17). This supports the specificity of our approach and confirms that the DRG resident macrophages proliferation is CSF1R-dependent.

SGCs have been shown to repopulate in DRG in inflammatory conditions such as monoarthritis (21). Our study identified its specific turnover after axotomy and also identified the likely involvement of Sox2. Sox2 was recognized as a survival factor for SGCs (22). In this study, Sox2 expression in $Ki67^+$ SGCs indicates its association with SGCs turnover. Sox2 expression was also recognized for Schwann cells sorting in injured peripheral nerves (16). We noted that rings of SGCs surround injured neurons in an orderly fashion clearly suggesting that sorting of SGCs occurs in axotomized DRGs. In vivo cell sorting requires concerted actions of intracellular and external cues. We believe that Sox2 may also mark SGCs that participate in in vivo sorting.

We noted an intimate contact between macrophages and SGCs in the adult DRG. One possibility for this intimate contact may be that macrophages offer structural support for sorting of SGCs. For example, macrophages accumulate earlier than SGC activation in injured DRG potentially preparing for ensuing roles in sorting. We also found that the processes of activated macrophages apparently extend out to SGCs in vivo and in vitro in an organized manner. In addition, macrophages were seen distributed adjacent to cells that express Sox2, the intracellular molecule known for its sorting function. Thus, by offering a structural support, macrophages may serve as the external cue for the sorting of SGCs. An alternate possibility for the intimate contact between SGCs and macrophages may

be that they act to prime each other for their concerted actions on injured neurons.

We noted apoptosis following the enhanced cytogenesis in DRGs. This indeed shows a controlled DRG milieu despite expansion and dedifferentiation of mature cells to a proliferating, and later, functional phenotype. We do not know whether apoptosis occurs selectively to functionally naive or competent mature cells, although selective phenotypic markers were expressed by those cells.

Although our study identified that DRG resident macrophages self-renew and expand locally, the contribution of infiltrating monocytes to the overall macrophages pool in axotomized DRGs cannot be excluded. Also, this study did not address whether monocyte infiltration precedes or follows local proliferation. A previous study showed local proliferation of endoneurial macrophages in injured peripheral nerves prior to monocyte infiltration (7).

Macrophages were initially recognized as essential for Wallerian or axonal degeneration of injured nerves. However, their exact function in injured DRGs is still unclear (23). This raised the need to explore the functional avenues of DRG resident macrophages. Previous reports showed that DRG resident macrophages accumulate selectively around injured large caliber neurons ($NF200^{+++}$ neurons) than small caliber C neurons ($NF200^{+}$ neurons), however, a functional significance for this selective accumulation is not known (8). We and others previously noted that DRG resident macrophages take up neuronal debris without inducing damage to neurons implying a role for cytoskeleton remodeling of neurons, possibly to rescue them from axotomy-induced DNA damage (1, 24, 25). On the other hand, detrimental roles for macrophages to human neurons have been reported in Friedreich ataxia and hippocampal sclerosis (26, 27). Given the identification and importance of multiple functional phenotypes of macrophages and their impact on remodeling the nervous system, the local proliferation of DRG resident macrophages that we report here requires further attention (9). Understanding the phenotypic destiny of the mitotic and nonmitotic subtypes of macrophages would identify specific intervention points for therapeutic trials related to nerve regeneration, inflammation and neuropathies generally. On the other hand, understanding the growth regulatory milieu of DRG in response to remote signals may also offer insights into the intrinsic trophic signals and their roles on closely related pathologies.

REFERENCES

1. Christie K, Koshy D, Cheng C, et al. Intraganglionic interactions between satellite cells and adult sensory neurons. Mol Cell Neurosci 2015; 67:1–12
2. Webber CA, Christie KJ, Cheng C, et al. Schwann cells direct peripheral nerve regeneration through the Netrin-1 receptors, DCC and Unc5H2. Glia 2011;59:1503–17
3. Krishnan A. Neuregulin-1 type I: a hidden power within Schwann cells for triggering peripheral nerve remyelination. Science Signaling 2013;6:jc1
4. Lu X, Richardson PM. Inflammation near the nerve cell body enhances axonal regeneration. J Neurosci 1991;11:972–8
5. Chen YS, Chung SS, Chung SK. Aldose reductase deficiency improves Wallerian degeneration and nerve regeneration in diabetic thy1-YFP mice. J Neuropathol Exp Neurol 2010;69:294–305
6. Zou T, Ling C, Xiao Y, et al. Exogenous tissue plasminogen activator enhances peripheral nerve regeneration and functional recovery after injury in mice. J Neuropathol Exp Neurol 2006;65:78–86
7. Mueller M, Wacker K, Ringelstein EB, et al. Rapid response of identified resident endoneurial macrophages to nerve injury. Am J Pathol 2001; 159:2187–97
8. Vega-Avelaira D, Geranton SM, Fitzgerald M. Differential regulation of immune responses and macrophage/neuron interactions in the dorsal root ganglion in young and adult rats following nerve injury. Mol Pain 2009; 5:70
9. Kroner A, Greenhalgh AD, Zarruk JG, et al. TNF and increased intracellular iron alter macrophage polarization to a detrimental M1 phenotype in the injured spinal cord. Neuron 2014;83:1098–116
10. Hashimoto D, Chow A, Noizat C, et al. Tissue-resident macrophages self-maintain locally throughout adult life with minimal contribution from circulating monocytes. Immunity 2013;38:792–804
11. Jenkins SJ, Ruckerl D, Cook PC, et al. Local macrophage proliferation, rather than recruitment from the blood, is a signature of TH2 inflammation. Science 2011;332:1284–8
12. Robbins CS, Hilgendorf I, Weber GF, et al. Local proliferation dominates lesional macrophage accumulation in atherosclerosis. Nat Med 2013;19:1166–72
13. Christie KJ, Krishnan A, Martinez JA, et al. Enhancing adult nerve regeneration through the knockdown of retinoblastoma protein. Nat Commun 2014;5:3670
14. Donegan M, Kernisant M, Cua C, et al. Satellite glial cell proliferation in the trigeminal ganglia after chronic constriction injury of the infraorbital nerve. Glia 2013;61:2000–8
15. Lee S, Zhang J. Heterogeneity of macrophages in injured trigeminal nerves: cytokine/chemokine expressing vs. phagocytic macrophages. Brain Behav Immun 2012;26:891–903
16. Parrinello S, Napoli I, Ribeiro S, et al. EphB signaling directs peripheral nerve regeneration through Sox2-dependent Schwann cell sorting. Cell 2010;143:145–55
17. Pyonteck SM, Akkari L, Schuhmacher AJ, et al. CSF-1R inhibition alters macrophage polarization and blocks glioma progression. Nat Med 2013; 19:1264–72
18. DeFrancesco-Lisowitz A, Lindborg JA, Niemi JP, et al. The neuroimmunology of degeneration and regeneration in the peripheral nervous system. Neuroscience 2015;302:174–203
19. Peng J, Gu N, Zhou L, et al. Microglia and monocytes synergistically promote the transition from acute to chronic pain after nerve injury. Nat Commun 2016;7:12029
20. Guan Z, Kuhn JA, Wang X, et al. Injured sensory neuron-derived CSF1 induces microglial proliferation and DAP12-dependent pain. Nat Neurosci 2016;19:94–101
21. Nascimento DS, Castro-Lopes JM, Moreira Neto FL. Satellite glial cells surrounding primary afferent neurons are activated and proliferate during monoarthritis in rats: is there a role for ATF3? PLoS ONE 2014;9: e108152
22. Koike T, Wakabayashi T, Mori T, et al. Sox2 promotes survival of satellite glial cells in vitro. Biochem Biophys Res Commun 2015;464:269–74
23. Krishnan A, Duraikannu A, Zochodne DW. Releasing 'brakes' to nerve regeneration: intrinsic molecular targets. Eur J Neurosci 2016;43: 297–308
24. Hu P, McLachlan EM. Distinct functional types of macrophage in dorsal root ganglia and spinal nerves proximal to sciatic and spinal nerve transections in the rat. Exp Neurol 2003;184:590–605
25. Krishnan A, Purdy K, Chandrasekhar A, et al. A BRCA1-dependent DNA damage response in the regenerating adult peripheral nerve milieu. Molec Neurobiol 2018;55:4051–67
26. Koeppen AH, Ramirez RL, Becker AB, et al. Dorsal root ganglia in Friedreich ataxia: satellite cell proliferation and inflammation. Acta Neuropathol Commun 2016;4:46
27. Lu JQ, Steve TA, Wheatley M, et al. Immune cell infiltrates in hippocampal sclerosis: correlation with neuronal loss. J Neuropathol Exp Neurol 2017;76:206–15